

Stripes and electronic quasiparticles in the pseudogap state of cuprate superconductors

Matthias Vojta

Institut für Theoretische Physik, Technische Universität Dresden, 01062 Dresden, Germany

(Dated: June 18, 2018)

This article is devoted to a discussion of stripe and electron-nematic order and their connection to electronic properties in the pseudogap regime of copper-oxide superconductors. We review basic properties of these symmetry-breaking ordering phenomena as well as proposals which connect them to quantum-oscillation measurements. Experimental data indicate that these orders are unlikely to be the cause of the pseudogap phenomenon, implying that they occur on top of the pseudogap state which itself is of different origin. Specifically, we discuss the idea that the non-superconducting pseudogap ground state hosts electron-like quasiparticles which coexist with a spin liquid, realizing a variant of a fractionalized Fermi liquid. We speculate on how stripe order in such a pseudogap state might offer a consistent description of ARPES, NMR, quantum-oscillation, and transport data.

I. INTRODUCTION

The field of cuprate high-temperature superconductors has seen remarkable experimental progress in recent years. However, many conceptual puzzles remain in interpreting the data, in particular when it comes to the non-superconducting state. One such puzzle concerns the character and origin of the so-called pseudogap regime in underdoped cuprates.^{1–3} Numerous proposals have been made to explain this apparent suppression of low-energy states below a doping-dependent pseudogap temperature T^* . These proposals include phase-incoherent Cooper pairing, other orders competing with superconductivity, exotic fractionalized states, and short-range singlet correlations as precursor to the half-filled Mott insulator.^{2,4} Experiments continue to shape and modify the community's view on the pseudogap regime, with some of the central recent results being the observation of quantum oscillations at low temperature and high magnetic field^{5–7} and the detection of various symmetry-breaking non-superconducting orders.

Among these orders, so-called stripe order^{9–12} takes a prominent role. Static spin and charge density modulations have not only been established^{13–15} to exist in the $\text{La}_{2-x}\text{Sr}_x\text{CuO}_4$ (or 214) family of cuprates, but they have also been detected in other families: Modulations in the charge sector, likely pinned by impurities, appear on the surface of $\text{Ca}_{2-x}\text{Na}_x\text{CuO}_2\text{Cl}_2$, $\text{Bi}_2\text{Sr}_2\text{CaCu}_2\text{O}_{8+\delta}$ and other Bi-based cuprates – as seen by scanning-tunnelling-microscopy (STM) techniques^{16–20} – and charge stripes have also been found in $\text{YBa}_2\text{Cu}_3\text{O}_y$ in high magnetic fields.²¹ Electron-nematic order, i.e., a breaking of lattice rotational symmetry, is often discussed in the context of stripes, as the melting of uni-directional modulations can naturally lead to a state with restored translation, but broken rotation symmetry.²² Indeed, for $\text{YBa}_2\text{Cu}_3\text{O}_y$ it has been argued that strong low-energy anisotropies in various experiments^{23–25} originate from the tendency toward electron-nematic order which enhances the weak orthorhombic crystalline anisotropy.^{26–28} Finally, there is by now accumulated evidence^{29–31} for a certain type

of loop-current order which breaks lattice inversion but preserves translation symmetry.³²

The fact that all these observations occurred in the pseudogap regime prompts to interrogate the relation between these symmetry-breaking orders and the pseudogap. In fact, recent theoretical proposals attempt to explain quantum-oscillation and (a subset of) transport data in the pseudogap regime in terms of Fermi-liquid-like quasiparticles moving in spin and charge-modulated states.^{8,33–40} However, a fully coherent picture has not yet emerged. On a broader scale, it is questionable that stripes account for the full pseudogap phenomenology. Alternatively, if the pseudogap state is of different origin, stripes should be investigated *on top* of this pseudogap state.

The purpose of this paper is twofold. First, we review salient properties of stripe and associated nematic states, and critically discuss current ideas on the emergence of Fermi pockets and their connection to quantum oscillations. Second, we discuss specific ideas^{41–45} for the pseudogap regime based on holes moving in a spin liquid with short-range magnetic order and connect them to the concept of fractionalized Fermi liquids.^{46,47} We then propose to model stripes utilizing a phenomenological form of the single-particle propagator in the pseudogap regime and analyze their properties.

In this article, the discussion will be mainly restricted to the non-superconducting state, and ideas on the pairing mechanism will not be covered. Similarly, loop-current order,^{32,48} albeit very interesting, will only be mentioned briefly.

A. Outline

The body of this paper is organized as follows: In Sec. II we introduce the stripe and related electron-nematic orders. Sec. III contains a general discussion on aspects of the cuprate pseudogap, together with current ideas on how stripe order on top of a Fermi-liquid-like state might explain experimental results from quantum-oscillation and transport measurements in the pseudo-

gap regime. Conceptual problems encountered in this description will lead us in Sec. IV to consider a different state underlying the pseudogap, namely a state where a spin-liquid background coexists with fermionic quasiparticles forming small Fermi pockets. This realizes a variant of a fractionalized Fermi liquid. Finally, Sec. V contains concrete calculations for stripes in a pseudogap state which itself is described by a phenomenological single-particle propagator accounting for the formation of hole pockets. We discuss to what extent these calculations can explain experimental observations. An outlook will close the paper.

II. STRIPE AND ELECTRON-NEMATIC ORDERS

Lattice-symmetry-breaking order in cuprates has been the subject of numerous review articles in the past.^{9–12} Here we concentrate on density-wave (or stripe) order – which breaks lattice translation symmetry and, in its uni-directional form, lattice rotation symmetry – and on so-called electron-nematic order, which breaks rotation but not translation symmetry. (In this liquid-crystal terminology, uni-directional density-wave order may also be called electron-smectic order.)

In this section we shall review both the relevant order parameters and their manifestation in various experimental probes.^{10,12,49}

A. Order parameters and symmetry breaking

Following Landau, ordered phases are best described in terms of order-parameter fields. In the following, we assume that the underlying crystal lattice is two-dimensional, with square-lattice (i.e. tetragonal) symmetry.

A charge density wave (CDW) is described by a pair of complex scalar fields ϕ_{cx}, ϕ_{cy} for the two CDW directions with wavevector \vec{Q}_{cx} and \vec{Q}_{cy} . The charge density (more generally, any observable which transforms as a scalar under spin rotations) is assumed to obey

$$\langle \rho(\vec{R}, \tau) \rangle = \rho_{\text{avg}} + \text{Re} \left[e^{i\vec{Q}_c \cdot \vec{R}} \phi_c(\vec{R}, \tau) \right]. \quad (1)$$

Similarly, a collinear spin-density wave (SDW) requires a pair of complex vector fields $\phi_{s\alpha x}, \phi_{s\alpha y}$, $\alpha = x, y, z$, with wavevectors \vec{Q}_{sx} and \vec{Q}_{sy} , such that the spin density follows

$$\langle S_\alpha(\vec{R}, \tau) \rangle = \text{Re} \left[e^{i\vec{Q}_s \cdot \vec{R}} \phi_{s\alpha}(\vec{R}, \tau) \right]. \quad (2)$$

Experimental results in 214 cuprates are consistent with uni-directional order, i.e., $\phi_{cx}, \phi_{s\alpha x} \neq 0$ and $\phi_{cy} = \phi_{s\alpha y} = 0$ or vice versa. The preferred wavevectors are $\vec{Q}_{sx} = 2\pi(0.5 \pm 1/M, 0.5)$, $\vec{Q}_{sy} = 2\pi(0.5, 0.5 \pm 1/M)$ and $\vec{Q}_{cx} = (2\pi/N, 0)$, $\vec{Q}_{cy} = (0, 2\pi/N)$, where M and N are

the doping-dependent real-space periodicities which follow $M = 2N$ to a good accuracy.^{10–13}

Given the propensity for uni-directional order, introducing a separate order parameter for rotational symmetry breaking in a tetragonal environment is useful:²² this is an Ising scalar ϕ_n for $l = 2$ spin-symmetric electron-nematic order which carries wavevector $\vec{Q} = 0$. ϕ_n may be defined from any spin-singlet observable which is even under time reversal and sensitive to real-space directions, like the bond kinetic energy,

$$\phi_n(\vec{r}, \tau) = \langle c_\sigma^\dagger(\vec{r}, \tau) c_\sigma(\vec{r}+x, \tau) - c_\sigma^\dagger(\vec{r}, \tau) c_\sigma(\vec{r}+y, \tau) \rangle. \quad (3)$$

It is common practice to refer to ϕ_n as nematic order parameter; note, however, that $\phi_n \neq 0$ in both nematic and smectic (stripe) phases. As discussed in Ref. 22, a nematic phase can occur as a precursor to stripe order, but nematic order unrelated to stripes has been discussed for the cuprates as well.²⁶ In some cuprates the tetragonal in-plane symmetry is broken down to orthorhombic, and spontaneous nematic order cannot exist. It may then still make sense to discuss the tendency toward electron-nematic order if a small microscopic anisotropy becomes strongly enhanced by electronic correlations.

Any of the above orders may co-exist with superconductivity, and arguments for both competition^{12,50–52} and cooperation^{53–55} of stripes and superconductivity have been put forward. While the anticorrelation between strong stripe order and high superconducting T_c and the field-induced enhancement of stripe order in superconducting compounds point towards competition,¹² the so-called antiphase superconductivity proposed⁵⁶ to explain the intriguing behavior of $\text{La}_{15/8}\text{Ba}_{1/8}\text{CuO}_4$ (Ref. 57) may point towards a more complex interplay of stripes and pairing.⁵⁸

B. Experimental signatures

A variety of experimental probes may be used to detect stripe and electron-nematic orders. Here we provide a brief list on theoretical expectations and corresponding experimental observations.¹²

Perhaps most importantly, broken translation symmetry arising from long-range density-wave order results in additional superlattice Bragg reflections in diffraction experiments. Those have been seen in 214 cuprates, both in the charge sector (using neutrons and X-rays) and in the spin sector (using neutrons).^{13–15} Static long-range charge order has not been seen in other compounds; weak incommensurate spin order is detected in very underdoped $\text{YBa}_2\text{Cu}_3\text{O}_y$ as well.⁵⁹ Static magnetic order has also been detected using μSR in both 214 and $\text{YBa}_2\text{Cu}_3\text{O}_y$ compounds, in both cases broadly consistent with the results from neutron scattering.

Spatial inhomogeneities, i.e., site differentiation in local quantities, have been detected using NMR and NQR, again in 214 and $\text{YBa}_2\text{Cu}_3\text{O}_y$ cuprates.¹² While most of this data could not be used to clearly infer an ordering

pattern, a very recent NMR experiment²¹ showed clear signatures of period-4 charge stripes in $\text{YBa}_2\text{Cu}_3\text{O}_y$ exposed to large magnetic fields. Furthermore, stripe-like inhomogeneities in the charge sector are seen in STM experiments on the surface of $\text{Bi}_2\text{Sr}_2\text{CaCu}_2\text{O}_{8+\delta}$ and $\text{Ca}_{2-x}\text{Na}_x\text{CuO}_2\text{Cl}_2$.^{16–19}

Broken translation symmetry also results – via Bragg scattering – in a reconstruction of the dispersion relation of any elementary excitation in the solid, and should therefore be visible, e.g., in single-electron and phonon spectra. Unfortunately, the experimental situation is not clear-cut, i.e., the backfolding of dispersions due to stripe order has not been unambiguously observed. This suggests that those effects might be weak and moreover masked by matrix-element effects. We note, however, that ARPES in stripe-ordered $\text{La}_{2-x-y}\text{Eu}_y\text{Sr}_x\text{CuO}_4$ has found some hints for reconstructed electron bands⁶⁰ (recall that the quality of ARPES data in 214 cuprates does at present not reach that of Bi-based cuprates). Also, various phonon anomalies have been detected and discussed in the context of stripe order.^{12,61}

Finally, sizeable stripe order can lead to a modulation of collective magnetism, in the extreme rendering it quasi-one-dimensional. The spin excitations of stripe-ordered $\text{La}_{15/8}\text{Ba}_{1/8}\text{CuO}_4$ (Ref. 62) indeed display an elevated-energy dispersion akin to that of spin ladders, and consequently models of coupled-spin ladders^{63,64} (or field-theoretic versions thereof⁶⁵) have been used to model the experimental data. Qualitatively similar results have also been obtained in a description of static stripes using the time-dependent Gutzwiller approximation to the one-band Hubbard model.⁶⁶

The broken rotation symmetry inherent to both unidirectional stripe and electron-nematic states will cause in-plane anisotropies of all direction or momentum-dependent properties, such as charge and heat transport, fluctuation spectra etc. However, these anisotropies will only be visible in macroscopic measurements in a mono-domain situation. The alternating layer distortions in the LTT phase of 214 compounds therefore preclude global anisotropies. In $\text{YBa}_2\text{Cu}_3\text{O}_y$ this is different, and temperature-dependent anisotropies both in transport coefficients^{23,24} and in magnetic fluctuation spectra²⁵ have been observed, supporting the idea that the small (global) crystalline anisotropy becomes enhanced by electron-correlation effects at low temperatures. We note that the expected orthorhombic Fermi-surface distortion has not been seen, but this may again be related to the rather low quality of ARPES data for $\text{YBa}_2\text{Cu}_3\text{O}_y$.

The anisotropic magnetic fluctuations discovered in neutron scattering on $\text{YBa}_2\text{Cu}_3\text{O}_{6.45}$ in the absence of static order²⁵ admit interpretations in terms of both genuine (stripe-free) nematic order^{67,68} and incipient (i.e. fluctuating) stripe order.^{65,69}

III. STRIPES, FERMI POCKETS, AND THE PSEUDOGAP

In this section, we discuss existing ideas on how stripe order could explain selected features of the pseudogap regime, in particular quantum-oscillation and transport data. We shall argue that the existing modelling is likely incomplete because stripe order alone cannot account for the full pseudogap.

A. Pseudogap in a nutshell

Experimental data characterizing the pseudogap regime of cuprate superconductors have seen a spectacular evolution over the last years.^{1,5} To set the stage, we start by summarizing the most important observations.

Most generally, the term “pseudogap” refers to a partial suppression of low-energy electronic states, as compared to what is expected from a metallic phase, upon cooling below a doping-dependent pseudogap temperature T^* . This suppression is seen in both thermodynamic and spectroscopic observables. Momentum-resolved measurements indicate that the electronic states in the so-called antinodal region near momenta $(0, \pm\pi)$ and $(\pm\pi, 0)$ are the ones which become strongly gapped, such that the Fermi surface is reduced to apparent “Fermi arcs”.⁷⁰ Based on recent photoemission experiments it has been argued⁷¹ that these arcs in fact represent the “front part” of Fermi pockets, whose area is possibly compatible with the hole doping level, and we will come back to this later.

Both T^* and the estimated size of the low-temperature antinodal pseudogap, Δ_{PG} , monotonically decrease with doping, in striking difference to the superconducting T_c . T^* has been suggested to extrapolate to the scale J of the magnetic exchange in the limit of zero doping, and to vanish either around optimal doping or at the overdoped end of the superconducting dome. It should be noted, however, that the definition of T^* is not unique but depends – to some extent – on the considered observable.

In underdoped cuprates, signatures of short-range antiferromagnetism arising from local moments are ubiquitous: This includes magnetic collective modes with large spectral weight^{72,73} and magnetism which is induced or enhanced by non-magnetic impurities (e.g. by small concentrations of Zn substituting for Cu).^{74–76} Conceptually, it is plausible to attribute these strong antiferromagnetic fluctuations to the proximity to the parent Mott-insulating state,⁴ where local moments and their spin-wave excitations determine the magnetic response.

Moreover, symmetry-breaking orders are frequently found in the pseudogap regime. Most prominent are stripes^{9–12} seen as long-range bulk order in 214 cuprates and as disorder-pinned order on the surface of, e.g., $\text{Bi}_2\text{Sr}_2\text{CaCu}_2\text{O}_{8+\delta}$ and $\text{Ca}_{2-x}\text{Na}_x\text{CuO}_2\text{Cl}_2$. The tendency towards stripe order can be enhanced by applying a magnetic field, such that stripe order can even be induced

in compounds where zero-field static order is absent.^{21,77} The most plausible interpretation of this effect is based on competing order parameters: The magnetic field acts to suppress superconductivity which in turn enhances competing order such as stripes.⁵² In addition to stripes, strong temperature-dependent global anisotropies signifying electron-nematic order have been detected in $\text{YBa}_2\text{Cu}_3\text{O}_y$.^{10,12} Lastly, a weak intra-unit-cell magnetic order has been detected in polarized neutron scattering in both $\text{YBa}_2\text{Cu}_3\text{O}_y$ and $\text{HgBa}_2\text{CuO}_{4+\delta}$,^{29–31} which has been attributed to circulating-current order of the type proposed by Varma.³² It is remarkable that these various competing orders have been observed essentially exclusively in the pseudogap regime, with interpretations to be discussed in Sec. III D below.

B. Quantum oscillations

Quantum oscillations, i.e., oscillations of thermodynamic and transport properties as function of $1/B$ where B is a large applied magnetic field, are known from standard metals where they are most easily understood in terms of a semiclassical quantization of cyclotron orbits. de Haas-van Alphen and Shubnikov-de Haas effects are described by the Lifshitz-Kosevich theory.⁷⁸ At $T = 0$, the observed oscillation frequency F can be related to the momentum-space area A enclosed by the orbit at the Fermi energy via

$$F = \frac{\hbar c}{2\pi e} A. \quad (4)$$

To date, quantum oscillations have been detected not only in overdoped $\text{Tl}_2\text{Ba}_2\text{CuO}_{6+\delta}$ (Ref. 79) – located outside the pseudogap regime and expected to resemble a conventional metal – but also in underdoped $\text{YBa}_2\text{Cu}_3\text{O}_y$ and $\text{YBa}_2\text{Cu}_4\text{O}_8$,^{80–82} i.e., well inside the pseudogap regime. Quantum oscillations have also been observed on the electron-doped side of the phase diagram,^{83,84} where the data have been found to be broadly consistent with a Fermi surface reconstructed by antiferromagnetic order with $\vec{Q} = (\pi, \pi)$.

The observation of quantum oscillations in weakly hole-doped cuprates is considered an important breakthrough in the field, because it was long believed that coherent electronic quasiparticles do not exist in the pseudogap regime – an absence that was hypothesized mainly because early photoemission experiments only detected broad features in the single-electron spectrum. The natural conclusion from the observation of quantum oscillations is the presence of coherent fermionic quasiparticles moving (in a semiclassical picture) along closed momentum-space orbits. In fact, experimental data are in favor of Fermi-liquid-like quasiparticles causing the oscillations.^{85,86} Accepting this interpretation, various proposals for “exotic” pseudogap phases (e.g. with full spin-charge separation or otherwise incoherent carriers) appear to be ruled out.

For the later discussion, a few details of the quantum-oscillation results need to be mentioned:^{6,7}

- (i) The observations are so far restricted to the YBCO family and a relatively narrow doping range, $0.09 < x < 0.125$ in $\text{YBa}_2\text{Cu}_3\text{O}_y$ and $x \approx 0.14$ in $\text{YBa}_2\text{Cu}_4\text{O}_8$. It is uncertain whether the disappearance of quantum oscillations outside this doping range indicates a distinct quantum phase transition (QPT)⁸⁷ or simply originates from lower sample quality.
- (ii) Converting the measured oscillation frequency of approximately 530 T into a momentum-space area using Eq. (4), one concludes that the carriers form Fermi pockets whose size is approximately 2% of the Brillouin zone. This pocket size increases with doping x , but slower than expected for a pocket area $\propto x$, see e.g. Fig. 5b of Ref. 6.
- (iii) Transport measurements detect a negative Hall constant in the regime where quantum oscillations occur, more precisely, in $\text{YBa}_2\text{Cu}_3\text{O}_y$ at large fields and low temperatures for all $x > 0.08$.^{88,89} In a Fermi-liquid-based picture, this suggests that quantum oscillations are caused by electron (instead of hole) pockets. (However, it has been argued from experimental data that electron-like transport may also arise from near-nodal states.⁹⁰)
- (iv) There is no consensus on the role of superconductivity in the quantum-oscillation experiments. Although the measurements are performed in a resistive state, pairing e.g. in a “vortex liquid” can still be strong. While most interpretations assume that the oscillations reflect the physics of the underlying normal state, it is also conceivable that a superconducting state features Fermi pockets^{58,91,92} which lead to quantum oscillations.

C. Fermi pockets from density waves

The small momentum-space area of the Fermi pockets deduced from quantum-oscillation data in underdoped cuprates [see point (ii) in Sec. III B above] has triggered explanations based on translation-symmetry breaking in a metallic normal state: Density-wave order reconstructs the underlying Fermi surface, such that multiple pockets can appear, whose individual is unrelated to the electron concentration (apart from an overall sum rule). Given that stripes are the most prominent form of density-wave order observed in the cuprates, it is plausible to connect Fermi pockets caused by stripe order (in the spin or charge channel) to quantum oscillations.

Concrete calculations are essentially all based on a mean-field description of the symmetry-breaking order on top of a conventional Fermi-liquid-like state. Most often^{33–40} the latter is simply modelled by free fermions

with a dispersion $\epsilon_{\vec{k}}$ and a “large” Fermi surface as derived from band-structure calculations. Then, the quasi-particle properties of the ordered state can be obtained

$$\begin{bmatrix} \epsilon_{\vec{k}} & V_c^* & 0 & V_c & 0 & V_s^* & V_s & 0 \\ V_c & \epsilon_{\vec{k}+(\frac{\pi}{2},0)} & V_c^* & 0 & 0 & 0 & V_s^* & V_s \\ 0 & V_c & \epsilon_{\vec{k}+(\pi,0)} & V_c^* & V_s & 0 & 0 & V_s^* \\ V_c^* & 0 & V_c & \epsilon_{\vec{k}+(\frac{3\pi}{2},0)} & V_s^* & V_s & 0 & 0 \\ 0 & 0 & V_s^* & V_s & \epsilon_{\vec{k}+(\frac{\pi}{4},\pi)} & V_c^* & 0 & V_c \\ V_s & 0 & 0 & V_s^* & V_c & \epsilon_{\vec{k}+(\frac{3\pi}{4},\pi)} & V_c^* & 0 \\ V_s^* & V_s & 0 & 0 & 0 & V_c & \epsilon_{\vec{k}+(\frac{5\pi}{4},\pi)} & V_c^* \\ 0 & V_s^* & V_s & 0 & V_c^* & 0 & V_c & \epsilon_{\vec{k}+(\frac{7\pi}{4},\pi)} \end{bmatrix}. \quad (5)$$

Here, V_c (V_s) are the scattering potentials implementing long-range charge (spin) stripe order. In general, V_c and V_s are complex and momentum-dependent, reflecting the real-space structure and symmetry of the order.^{34,35,37,93} However, in most cases the Fermi surface depends only weakly on the precise form of V_c and V_s , which are therefore often approximated as real constants.

Uni-directional spin stripes have been found to produce electron pockets in the reconstructed Fermi surface^{35,36} which are formed out of antinodal electronic states. These electron pockets have been proposed as explanation for the simultaneous occurrence of quantum oscillations and a negative low-temperature Hall coefficient in $\text{YBa}_2\text{Cu}_3\text{O}_y$ over a certain range of dopings.⁸⁹ In this scenario, reducing the doping level may eventually lead to a Lifshitz transition where the electron pockets merge and disappear in favor of open orbits.³⁶

Sample results, which are qualitatively similar to those published in Refs. 34–37, are shown in Figs. 1 and 2. To facilitate comparison to the results in Sec. V below, the dispersion is taken from renormalized mean-field theory,⁴² $\epsilon_{\vec{k}} = -2t(\cos k_x + \cos k_y) - 4t' \cos k_x \cos k_y - 2t''(\cos 2k_x + \cos 2k_y)$ with $t_0 = 0.3 \text{ eV}$, $t'_0 = -0.3t_0$, $t''_0 = 0.2t_0$ and renormalized hopping amplitudes $t = g_t(x)t_0 + 3g_s(x)J\chi/8$, $t' = g_t(x)t'_0$, $t'' = g_t(x)t''_0$, where $\chi = 0.338$ and the Gutzwiller factors are $g_t(x) = 2x/(1+x)$, $g_s(x) = 4/(1+x)^2$.

Comparing Figs. 1 and 2 it is obvious that the area of all Fermi pockets is determined by an interplay of doping level, stripe period, and stripe strength and thus depends on microscopic details. The disappearance of the antinodal electron pockets happens due to the doping dependence of the spatial modulation period, which is assumed here to be similar to that of 214 cuprates.⁹⁴ It should be noted that, in addition to electron pockets, near-nodal hole pockets as in Figs. 1 and 2 occur quite generically in such stripe models. It has been suggested that the signatures of these pockets in quantum-oscillation and Hall measurements might be weak due to a low carrier mo-

bility, but we are not aware of a satisfactory explanation of the latter. A related problem may be that high-field specific-heat measurements⁹⁵ find a rather small value of $\gamma = C/T$, which appears incompatible with multiple Fermi sheets as in Figs. 1b,c and 2b,c.

Based on some analogies between 214 and $\text{YBa}_2\text{Cu}_3\text{O}_y$ cuprates, it has been suggested that the Fermi-surface reconstruction by stripe order is a general phenomenon, being responsible for a number of thermodynamic and transport anomalies.^{96,97} While stripe order indeed appears to be realized in both cuprate families, we believe that care is required when it comes to ideas about “fluctuating stripe order”. Given that d.c. transport and quantum oscillations are essentially static probes, they will *not* be influenced by temporally fluctuating stripe order. In other words, only static order with sufficiently large correlation length can be expected to leave signatures in transport coefficients. (This is different for a finite-energy probe like inelastic neutron scattering which is sensitive to fluctuating stripes.⁶⁵)

A few alternative proposals for density-wave order deserve to be mentioned, which were partially motivated by (a) the apparent lack of strong spin order^{21,25,59} in $\text{YBa}_2\text{Cu}_3\text{O}_y$ for $0.09 < x < 0.14$ and (b) the problem of invoking low-energy antinodal states for the pockets which, however, are believed to be strongly gapped in the pseudogap regime. Ref. 38 combined charge-only stripe order with a sizeable nematic distortion of the Fermi surface and obtained electron pockets for $x = 1/8$, however, an account of the doping dependence was not given. In contrast, Ref. 40 proposed bi-directional charge order which may yield electron pockets formed out of nodal electron states. It remains open how this proposal can be compatible with the results of scattering and NMR experiments.

We will return to this set of ideas and their conceptual aspects in Sec. III E below.

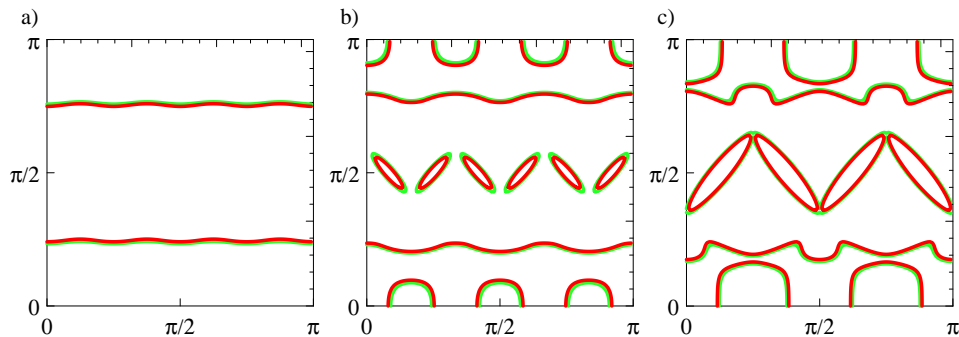


FIG. 1: Doping evolution of Fermi surfaces (dark red) for vertical spin stripes, shown in a quadrant of the Brillouin zone. The stripe strength decreases with doping: a) $x = 1/16$, $M = 16$, $V_s = 0.04$ eV. b) $x = 1/12$, $M = 12$, $V_s = 0.03$ eV. c) $x = 1/8$, $M = 8$, $V_s = 0.02$ eV. In all cases, weak charge order is added with $V_c = V_s/10$ and $N = M/2$. The light green lines are constant-energy contours at small negative energy to indicate the dispersion gradient. From b) to a) a Lifshitz transition occurs where the antinodal electron pockets disappear (the near-nodal hole pockets disappear as well). For further details see text.

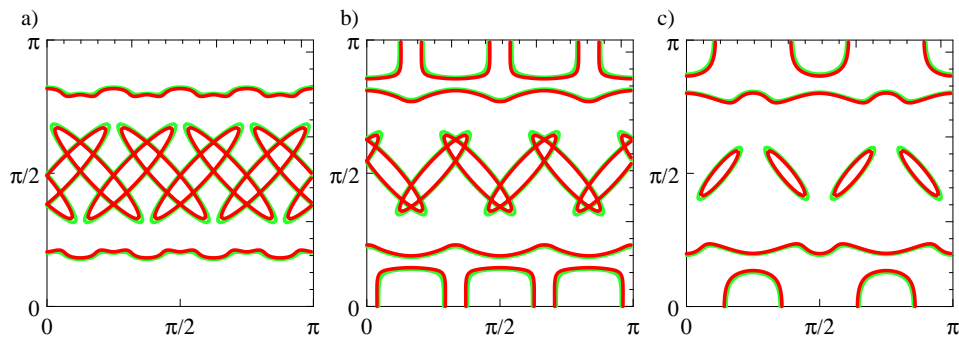


FIG. 2: Same as Fig. 1, but now the stripes are strongest at $x = 1/8$: a) $x = 1/16$, $M = 16$, $V_s = 0.015$ eV. b) $x = 1/12$, $M = 12$, $V_s = 0.02$ eV. c) $x = 1/8$, $M = 8$, $V_s = 0.03$ eV. The near-nodal hole pockets exist for all doping levels.

D. Scenarios for the pseudogap

The presentation so far prompts to ask for the relation between stripe order and the pseudogap phenomenon, urging to discuss the origin of the latter. Given that the list of proposed explanations for the pseudogap is long, I will restrict this section to a summary of the most influential suggestions.

One class of ideas describes the pseudogap as a precursor of superconductivity, i.e., the suppression of fermionic DOS happens because of phase-incoherent Cooper-pair formation. Indeed, signatures of preformed pairs above T_c ⁹⁸ have been identified in a number of experiments, most notably Nernst effect measurements,⁹⁹ but also in photoemission,^{100,101} and STM studies.¹⁰² This interpretation is supported by the observation of fluctuating diamagnetism which often varies in proportion to the Nernst coefficient.¹⁰³ However, the experimental onset temperature of pairing fluctuations is significantly below the T^* established from other probes. This casts strong doubts on the assumption of preformed pairs being the primary source of the pseudogap.

A second class ascribes the pseudogap to an ordering phenomenon which competes with superconductivity. The vanishing of the corresponding ordering temperature upon increasing the doping level naturally induces a quantum critical point (QCP) on the doping axis, which could be made responsible for anomalous normal-state properties. Among the concrete proposals for such competing phases are stripe^{104,105} and electron-nematic²² phases as well as circulating-current orders.^{32,48} One objection against these proposals is that the pseudogap line at T^* does not appear to be associated with a thermodynamic phase transition. However, this can be circumvented either by invoking quenched disorder which tends to smear the transition or by postulating a special form of phase transition with weak thermodynamic singularities, e.g. of Kosterlitz-Thouless or Ashkin-Teller type¹⁰⁶. In fact, a weak but sharp signature in the uniform susceptibility has recently been detected in YBCO samples of different doping, tracking the pseudogap temperature.¹⁰⁷ A second objection concerns the momentum-space structure of the gap: a finite- \vec{Q} order parameter (like stripes) causes gaps to appear near certain hot spots, but this

is inconsistent with the apparent d -wave nature of the pseudogap.¹ A third objection, perhaps most serious, concerns universality: The pseudogap appears to be a universal phenomenon in hole-doped cuprates, with very similar properties in the different families, which suggests a common origin. In contrast, stripes are strongest in single-layer compounds of the 214 family, but are weak or absent, e.g., in materials with more than two CuO_2 layers per unit cell. A similar objection may also apply to loop-current order at $\bar{Q}=0$, with their signatures detected in a subset of cuprate families only. Finally, while microscopic calculations using cluster extensions of dynamical mean-field theory (DMFT), to be discussed in more detail in Sec. IV C below, have established the existence of a pseudogap in the 2d Hubbard model,^{108–112} this pseudogap occurs in the *absence* of long-range order. This suggests that long-range order is not required for pseudogap formation.

A conceptual remark is in order: A particular symmetry-breaking order being the origin of the pseudogap obviously explains why this order is only seen below T^* , while discarding such a pseudogap explanation would imply that the various symmetry-breaking orders are a result (rather than the cause) of the pseudogap. (A recent detailed analysis of STM data from $\text{Bi}_2\text{Sr}_2\text{CaCu}_2\text{O}_{8+\delta}$ concluded that stripes are unlikely to be the cause of the pseudogap.¹⁹)

We are lead to a third class of ideas, relating the pseudogap to strong correlations and the proximity to the parent Mott insulator, without invoking symmetry breaking. While a satisfactory phenomenological description of these ideas is lacking to date, the theoretical results can be grouped into (i) numerical results from cluster extensions of DMFT, which suggest that short-range singlet formation may be responsible for a partial gap formation,^{108–112} (ii) corresponding field theories trying to formalize “Mottness”,¹¹³ and (iii) proposals based on low-energy theories for exotic phases involving fractionalization. Such proposals also imply the existence of a QCP on the doping axis (marking a transition between the underdoped exotic and the overdoped Fermi-liquid phase), but here *without* symmetry breaking on either side of the phase diagram. One concrete such proposal will be the subject of Sec. IV below.

E. Conceptual problems of Fermi-liquid based stripes

Clearly, identifying the origin of the pseudogap also has immediate consequences for the proposed explanations for quantum-oscillation experiments. A key question is whether a conventional Fermi-liquid-based description of the symmetry-breaking orders is justified. While the quantum-oscillation data itself suggest that the answer might be “yes”, the temperature evolution of both thermodynamic and spectral properties in the pseudogap regime¹ appears inconsistent with this assumption.

A generally accepted solution of this puzzle is not known to date, but two alternatives are obvious:

- (A) The low-doping state is asymptotically a conventional Fermi liquid (in the absence of superconductivity), but with both coherence temperature and quasiparticle weight being small. This implies, e.g., that the underlying Fermi surface of this state is “large”, i.e., it fulfills Luttinger’s theorem (see Sec. IV for a more detailed discussion). This large Fermi surface may be unobservable if translational symmetry breaking sets in above the coherence temperature.
- (b) The low-doping state is a metallic non-Fermi liquid which features coherent fermionic quasiparticles, but is *not* a Fermi liquid because Luttinger’s theorem is violated. Such a state can be classified as fractionalized Fermi liquid,⁴⁶ discussed in detail in Sec. IV. Most plausibly, the Fermi surface consists of hole pockets,^{44,45} with a total area given by the doping level x – this appears supported by cluster DMFT studies.¹¹² A phenomenological ansatz for the self-energy describing a pseudogap state with small pockets has been put forward independently in Ref. 42.

To date, photoemission experiments have not been able to distinguish the available scenarios, mainly because of insufficient energy and momentum resolution (although progress has been made recently^{71,114}).

Most theoretical models to explain the quantum-oscillation frequencies in underdoped cuprates operate with density-wave order occurring on top of a Fermi-liquid state with weakly interacting quasiparticles and a large Fermi surface. Apparently, these models are heavily based on scenario (A). Taking the models of Refs. 34,36 and others at face value, a number of problems are apparent:

- (1) The single-particle states which form the electron pockets stem from the antinodal portion of the Brillouin zone where, however – according to ARPES – a large gap exists. While this argument may be flawed because it is comparing the high-field low-temperature regime of quantum oscillations with the zero-field elevated-temperature regime of ARPES, the more general problem is that a stripe modulation on top of a large Fermi surface does not account for the pseudogap (e.g. because it cannot explain the momentum-space structure of the pseudogap).
- (2) Stripe order leads, in addition to the desired electron pockets, to further sheets of Fermi surface (both open orbits and hole pockets). Their existence appears to be in conflict with high-field specific-heat data: The small measured value of γ suggests that the pockets seen in quantum oscillations reflect the only gapless charge carriers in the system.⁹⁵

- (3) In most calculations, sizable spin stripe order is required to produce electron pockets while charge order alone leads to hole pockets only. However, a recent NMR experiment on $\text{YBa}_2\text{Cu}_3\text{O}_y$ suggests that spin order is not present (or very weak) in the regime of interest.²¹ Charge stripes on top of a nematic state have been suggested to resolve this conflict.³⁸
- (4) The weakly doping-independent area of the pocket in the doping range $0.09 < x < 0.14$ for $\text{YBa}_2\text{Cu}_3\text{O}_y$ and $\text{YBa}_2\text{Cu}_4\text{O}_8$ requires fine tuning in essentially all models, perhaps with the exception of the bi-directional charge modulation proposed in Ref. 40.

Clearly, the conceptual problem (1) appears most pressing. This prompts to consider scenario (B), i.e., a non-Fermi liquid pseudogap state, on top of which stripe order may occur. This is discussed in the remainder of the article.

IV. FRACTIONALIZED FERMI LIQUIDS AND THE PSEUDOGAP

We now turn to an appealing scenario for the pseudogap ground state, which invokes a non-Fermi liquid which nevertheless features well-defined fermionic quasiparticles. Such a state is best classified as a “fractionalized Fermi liquid” (FL^{*}). This term, originally introduced in the context of heavy-fermion systems, refers to a metallic phase without spontaneously broken symmetries in which sharp quasiparticles (with spin 1/2 and charge e) coexist with a paramagnetic spin liquid.¹¹⁵

We begin by reviewing the concepts of fractionalized Fermi liquids and the related orbital-selective Mott transitions for two-band systems (like heavy fermions) and then discuss the application of these ideas to weakly doped (one-band) Mott insulators. This will eventually lead us to propose the phase diagram in Fig. 3, where a fractionalized Fermi liquid at low doping and a conventional Fermi liquid at high doping are separated by a QPT.

A. Orbital-selective Mott phases and fractionalized Fermi liquids in two-band systems

Loosely speaking, an orbital-selective (or band-selective) Mott phase – dubbed OS Mott in the following – is a metallic phase of a two-band system, where one band (dubbed c in the following) is “metallic” (with Fermi-liquid-like quasiparticles), while the other (f) is “Mott-insulating” as a result of strong electronic correlations. (The generalization to more than two bands is straightforward.) The electrons in the Mott-insulating band form local moments, which may either order magnetically or

settle in a non-magnetic spin-liquid state at low temperatures. As will be argued below, a spin-liquid ground state of the local moments is required to define a fractionalized Fermi liquid.

A sharp distinction between a band being metallic or Mott-insulating can be made by considering the momentum-space volume enclosed by the Fermi surface: here a metallic band contributes, whereas a Mott-insulating band does not. In a standard Fermi-liquid (FL) phase of a two-band system, both bands are metallic in the above sense, and the Fermi volume is given by

$$\mathcal{V}_{\text{FL}} = K_d(n_{\text{tot}} \bmod 2). \quad (6)$$

Here $n_{\text{tot}} = n_c + n_f$ denotes the number of electrons per unit cell, $\bmod 2$ implies that full bands are not counted, $K_d = (2\pi)^d / (2v_0)$ is a phase space factor, with v_0 the unit cell volume, and the factor of 2 accounts for the spin degeneracy of the bands. Importantly, the “large” Fermi volume of Eq. (6) is in accordance with Luttinger’s theorem.¹¹⁶

The key point is now that an OS Mott phase has a Fermi volume *different* from \mathcal{V}_{FL} (6) because the electrons of the Mott-insulating band do not contribute. As the number of electrons *per site* corresponding to a Mott-insulating band is unity, n_{tot} in Eq. (6) is replaced by $(n_{\text{tot}} - N_{\text{cell}})$, which yields a distinct Fermi volume if the number of sites per unit cell, N_{cell} , is odd (and spin degeneracy is preserved). Therefore, a sharp definition of an OS Mott phase requires that the local moments of the Mott-insulating band are in a spin-liquid state without spontaneously broken symmetries – such a state typically features fractionalized spin excitations. Hence, we arrive at a phase where conduction electrons coexist with a fractionalized spin liquid – this is exactly what was dubbed “fractionalized Fermi liquid” in Ref. 46. Its Fermi volume is “small”,

$$\mathcal{V}_{\text{FL}^*} = K_d[(n_{\text{tot}} - 1) \bmod 2], \quad (7)$$

and violates the Fermi-volume count according to Luttinger’s theorem exactly by unity, hence this FL^{*} phase is a true non-Fermi liquid metal. It is separated from FL by a quantum phase transition dubbed “orbital-selective Mott transition”, where the Fermi volume changes discontinuously.

If, in contrast, the local moments in the OS Mott regime realize a symmetry-broken state as $T \rightarrow 0$, be it an antiferromagnet or a valence-bond solid, the unit cell is enlarged, and the sharp distinction between small and large Fermi volumes is lost (because the two states only differ in the number of *full* bands). Consequently, the resulting local-moment phase may be adiabatically connected to a fully itinerant broken-symmetry Fermi liquid.¹¹⁷

FL^{*} phases can be readily constructed in the framework of Kondo-lattice models.^{46,47} Start from a spin-only system with single-site unit cell and geometric frustration, such that a spin-liquid state is realized. Can-

didates are spin-1/2 magnets on the Kagome or pyrochlore lattices as well as e.g. triangular or square lattices with longer-range or multiple spin-exchange interactions.^{118–120} Then, add conduction electrons and couple those via a (weak) Kondo coupling to the spin liquid. As the spin liquid is a stable state of matter, a weak Kondo coupling is irrelevant in the RG sense, hence the properties of the two subsystems will remain qualitatively unchanged, and a FL* phase naturally emerges. (This is particularly obvious if the spin liquid is gapped.) Hence, in the Kondo limit the existence of FL* phases in two-band systems only rests upon the existence of fractionalized spin liquids in frustrated magnets. In this limit $n_f \equiv 1$, and $\mathcal{V}_{\text{FL}^*}$ (7) is given by n_c only. The OS Mott transition between FL* and FL can be understood as breakdown of Kondo screening of the local moments which happens due to the competition between Kondo effect and non-local inter-moment correlations.^{46,121–123} (In transition-metal oxides realizing multiband Hubbard systems, an additional driver for OS Mott physics is Hund’s-rule coupling which counteracts the screening of local moments.^{115,124}

We note that, in principle, different flavors of FL* phases can exist, depending on the nature of the spin-liquid component (gapped, gapless, Z_2 or $U(1)$ gauge forces). However, the full systematics of FL* phases, including the fate of topological order in the presence of charge carriers, is not understood to date.

B. Application to weakly doped Mott insulators

Various phenomenological aspects of underdoped cuprates suggest an interpretation in terms of a fractionalized Fermi liquid, where hole-like charge carriers coexist with a spin-liquid background. This thinking goes back to Anderson’s early idea of a resonating valence-bond state doped with holes^{41,125} and has been subsequently reformulated in various flavors.^{42–45,128–130}

A number of conceptual ideas are naturally account for: (i) local moments inherited from the parent Mott insulator continue to exist in the weakly hole-doped FL* state, (ii) the charge-carrier density in this weakly doped Mott insulator is small (i.e. given by the number of doped holes instead of the total number of electrons), and these carriers may form small hole pockets, (iii) the low-doping phase cannot be adiabatically connected to a Fermi liquid with a large Fermi surface, but instead a QPT occurs on the doping axis, which in turn may be responsible for extended non-Fermi-liquid behavior around optimal doping above T_c , (iv) electronic states in certain momentum-space regions (where only the large Fermi surface would exist) will disappear at low energy and temperature in the low-doping FL* phase, thereby creating a pseudogap, and (v) a superconducting state formed at low doping will display a pairing gap on the small Fermi surface of FL* which coexists with the pseudogap. Apparently, this list bears striking similarity with experimental observations

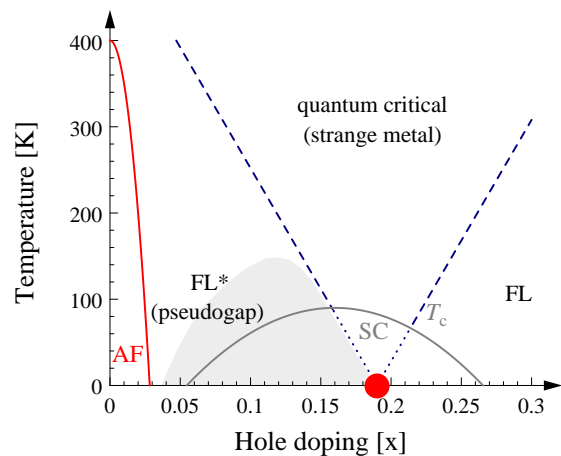


FIG. 3: Hypothesized phase diagram for hole-doped cuprates in the temperature–doping plane, with a quantum critical point (●) separating the overdoped FL and the underdoped FL* phase – the latter represents the pseudogap, which itself may host various forms of competing order (shaded). The finite-temperature quantum critical regime of the FL–FL* transition is cut-off below T_c by superconductivity. Also shown is the onset of commensurate antiferromagnetism (AF); not shown are additional crossovers associated with the onset of pairing fluctuations and with spin-glass behavior.

in cuprates.

Given the precise definition of a fractionalized Fermi liquid phase in a two-band system, it is natural to ask how this concept can be adapted to a one-band doped Mott insulator.¹³¹ It is plausible to start again from an undoped Mott insulator, where magnetic order is suppressed by quantum fluctuations or frustration, such that a fractionalized spin liquid is realized. A possible candidate state is an RVB-like state with short-range correlations. In contrast to the two-band case, charge carriers are now added in the *same* band by doping holes. *If* these holes retain their integrity, i.e., continue to exist as elementary excitations of spin 1/2 and charge e with a Fermi surface, then an FL* phase is realized: These quasiparticles co-exist with a spin liquid, and the volume of the *hole* Fermi surface is given by the hole concentration x , whereas Luttinger’s theorem would dictate a Fermi volume of $(1-x)$ electrons or, equivalently, $(1+x)$ holes. Hence, the Luttinger count is violated exactly by unity as in the two-band situation discussed above.¹³²

A conceptual problem of this idea is that carrier doping of a fractionalized spin liquid will – quite generically – lead to a fractionalization of the doped carriers, i.e., a doped hole will decay into a neutral spinon (as this is a good quasiparticle of the background spin liquid) and a charged spinless holon.^{125–127} The key idea to circumvent this problem is via the formation of *bound states*. Imagine a fractionalized state in which a spinon and a holon can form a low-energy bound state. This bound state is equivalent to a hole, and particles occupying these bound

states will feature a Fermi surface, with properties as described above. As a spin-off, spinon-spinon bound states are possible as well, leading to sharp low-energy resonances in neutron scattering. Importantly, such an FL* state will display bound-state holes and fractionalization at the same time, such that low-energy observables will often see signatures of sharp quasiparticles while experiments at higher energy will detect continua characteristic of fractionalization.

Interestingly, the idea of spinons and holons undergoing “reconfinement” to form a conventional quasiparticle was already discussed in the 1990s based on numerical results for the $t - J$ model.¹²⁸ A phenomenological ansatz for a Green’s function describing quasiparticles with hole pockets was proposed by Yang, Rice, and Zhang;⁴² its form can be related to bound-state formation of holons and spinons in a mean-field RVB spin liquid. More recently, Sachdev and co-workers^{44,45} studied the dynamics of electrons in a fluctuating 2d antiferromagnet. This first leads to the emergence of an algebraic charge liquid,¹²⁹ with separate excitations for spin and charge. Those were proposed to form bound states, i.e., electrons with a pocket-like Fermi surface. A clear connection to FL* phases was then made in Ref. 45. In this scenario, the spin-liquid component is gapless and derived from local AF order, instead of the short-range RVB state advocated above. Finally, Ref. 130 also proposed a metallic state with hole pockets for the pseudogap, which was dubbed a Luttinger-volume-violating Fermi liquid. It derives again from a RVB-like spin-liquid state, where the doped hole retain their integrity. In line with the above discussion, this state can be labelled fractionalized Fermi liquid as well.

C. Numerical evidence

Computer simulations of the 2d Hubbard model^{110–112,134–137} using cluster extensions of DMFT¹³⁸ have provided insight into the physics of weakly doped Mott insulators. Among other things, these calculations show pseudogap behavior at low doping in the absence of superconductivity or magnetic order.

In the single-particle Green’s function, this pseudogap behavior is accompanied by the disappearance of the Fermi surface in parts of the Brillouin zone, namely in the antinodal regions near $(\pi, 0)$, $(0, \pi)$ ^{111,112,135–137}. This low-doping behavior is found to be qualitatively distinct from that at high doping, with a regime of strong scattering in between, suggestive of a quantum phase transition.^{110,134} These results bear remarkable resemblance to those from photoemission experiments on actual cuprates. Because of the similarity to orbital-selective Mott physics, the partial disappearance of the Fermi surface upon decreasing the doping has been termed “momentum-selective Mott transition”.

This lends support to a phase diagram as in Fig. 3, where a non-Fermi liquid phase is realized at low doping,

which is separated by a QPT from a Fermi liquid at large doping. In fact, a detailed analysis and extrapolation of the cluster-DMFT self-energies and spectral functions in the low-doping regime has uncovered that the underlying Fermi surface consists of the proposed four pockets.¹¹² However, the detailed nature of the accompanying spin-liquid state has not been understood in phenomenological terms to date.

D. Single-particle propagator in the pseudogap phase

While a complete theory for a one-band FL* is not available at present, concrete proposals have been made for approximate forms of the single-electron Green’s function in the putative zero-temperature normal state describing the pseudogap. These include the phenomenological ansatz by Yang, Rice, and Zhang (YRZ, Ref. 42) and the effective model of Qi and Sachdev (QS, Ref. 44) for bound-state formation in an algebraic charge liquid.

Although the underlying physical ideas are somewhat different, both proposals can be written in terms of the following single-particle propagator

$$G(\vec{k}, \omega) = \frac{Z}{\omega - \xi_{\vec{k}} - \Delta_{\vec{k}}^2 / (\omega - \xi'_{\vec{k}})} \quad (8)$$

defined on the microscopic square lattice. Here $\xi_{\vec{k}}$ is a single-particle dispersion leading to a large Fermi surface, such that the large-doping FL state is described by $\Delta_{\vec{k}} = 0$, and Z is a (doping-dependent) weight factor. In the YRZ proposal, the individual terms are given by

$$\begin{aligned} \xi_{\vec{k}} &= \epsilon_{\vec{k}} - \mu, \\ \xi'_{\vec{k}} &= 2t(\cos k_x + \cos k_y), \\ \Delta_{\vec{k}} &= \Delta(x)(\cos k_x - \cos k_y), \end{aligned} \quad (9)$$

with $\epsilon_{\vec{k}} = -2t(\cos k_x + \cos k_y) - 4t' \cos k_x \cos k_y - 2t''(\cos 2k_x + \cos 2k_y)$. Physically, $\xi'_{\vec{k}}$ reflects a nearest-neighbor “spinon” dispersion, while the d -wave form of the gap $\Delta_{\vec{k}}$ arises from an implicit pairing assumption. In contrast, the QS scenario yields

$$\begin{aligned} \xi_{\vec{k}} &= \epsilon_{1\vec{k}} + \epsilon_{2\vec{k}} - \mu, \\ \xi'_{\vec{k}} &= \epsilon_{1,\vec{k}+\vec{Q}} - \epsilon_{2,\vec{k}+\vec{Q}} - \mu, \\ \Delta_{\vec{k}} &= \Delta. \end{aligned} \quad (10)$$

Here, Δ measures the strength of local antiferromagnetic order, and $\epsilon_{1\vec{k}}$ and $\epsilon_{2\vec{k}}$ are the effective dispersions of the bound states between the two species of spinless fermions and bosonic spinons which appear in the algebraic charge liquid. Interestingly, this “fermion doubling” reflects the topological order of the underlying spin liquid.⁴⁴

For finite $\Delta_{\vec{k}}$, Eq. (8) leads to hole-pocket Fermi surfaces as shown in Fig. 4, with the exact shape and location being somewhat different in the YRZ and QS approaches. Both proposals require that, for $\Delta_{\vec{k}} \neq 0$, the

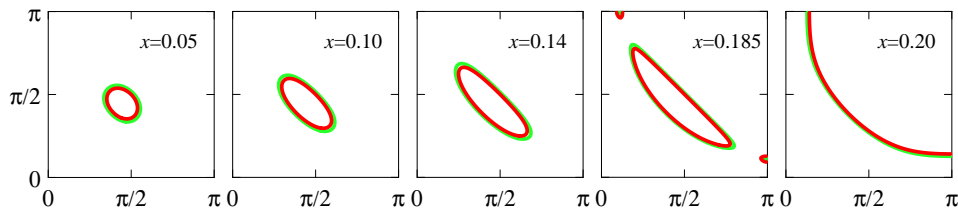


FIG. 4: Fermi surfaces in the pseudogap state as described by the YRZ ansatz (8,9) for different doping levels. For $x \lesssim 0.18$ only the lower YRZ band crosses the Fermi level, leading to one hole pocket per quadrant of the Brillouin zone. For $x > x_c = 0.2$ the large Fermi surface is recovered.

hole area enclosed by the Fermi pockets is given x holes, i.e., the *electron* area is $(2 - x)$, such that the Fermi-volume count violates Luttinger's theorem by unity. In both cases, a line of zeroes of G emerges where $\xi_{\vec{k}}^{\pm} = 0$ – note that this coincides with the antiferromagnetic zone boundary, $|k_x| + |k_y| = \pi$, only in the YRZ case.¹³²

In comparison to experiments, the Fermi surfaces derived from the YRZ ansatz have been argued to be in good agreement with pockets deduced from recent ARPES results,⁷¹ and agreement with other thermodynamic and spectroscopic observables has been suggested as well.⁴³ On the theoretical side, an analysis of the electronic self-energy obtained from small-cluster diagonalization of the Hubbard model has found the YRZ ansatz to be a reasonable approximation of the data.¹³⁹ Taken together, this suggests that an ansatz of the form (8) is an appropriate starting point in order to model symmetry-breaking orders in the pseudogap regime.

V. STRIPES IN THE PSEUDOGAP REGIME

From the discussion above, it appears plausible to take a different route in modelling electronic properties of stripes, namely to add stripe modulations on top of a pseudogapped ground state. In the absence of a complete theory of the latter, it is suggestive to combine the proposed forms of the single-particle propagator in a FL* state (YRZ or QS, see Sec. IV B) with a mean-field description of stripe order – this is what we will discuss in the following. To explore the connection to quantum oscillations and transport, we exclusively concentrate on the Fermi surface of such a stripe state.

To be specific, we employ the YRZ propagator, Eqs. (8,9), which can be written as a sum of two coherent quasiparticle poles at energies $E_{\vec{k}}^{\pm}$, dubbed upper and lower YRZ band. In the relevant doping range, the upper YRZ band lies far above the Fermi level⁴³ and can thus be ignored. Hence, we consider quasiparticles in the lower YRZ band which undergo stripe order. (This is similar in spirit to the treatment of superconductivity in the YRZ pseudogap state in Ref. 140 which considered pairing of the lower-band YRZ quasiparticles only.) At the mean-field level, stripe order is captured by Bragg scattering

terms which connect \vec{k} and $\vec{k} + \vec{Q}$ as usual, such that we are lead to diagonalize a matrix as in Eq. (5), where the bare energies are replaced by $E_{\vec{k}}^{\pm}$. Momentum-dependent weight factors of the YRZ quasiparticles are ignored at this level, but those will only have a minor influence on the Fermi surface.

We now turn to the results of this approach. We have chosen numerical parameters for the dispersion as in Sec. III C, and the YRZ hybridization is given by $\Delta(x) = \Delta_0(1 - x/x_c)$ with $\Delta_0 = t_0/2$ and $x_c = 0.2$.⁴² Sample Fermi surfaces are shown in Figs. 5 and 6, for the cases without and with spin order, respectively. The scattering potentials have been chosen to be moderate to strong, leading to relative doping modulations of order unity, to better visualize hybridization effects and pocket formation.

As is clearly visible, modulations on top of a hole-pocket state lead, depending on microscopic parameters, to a Fermi-surface reconstruction into hole pockets of different sizes and/or open orbits. The pockets are generically rather small and, by construction, emerge from near-nodal states. It appears, however, essentially impossible to generate electron pockets in this approach – both with and without spin order – because all low-energy bands are weakly hole-doped. Also, most Fermi-surface deformations arise from the hybridization between equal-spin bands, i.e., from charge order or from secondary spin-order effects. Quantitatively, the area of the small pockets in Fig. 5 (Fig. 6c) ranges between 0.6...1% (1.6%) of the full Brillouin zone, the large pockets in Fig. 5b have a size of approximately 4% of the full Brillouin zone.

From these results we conclude that stripe order on top of a pseudogap state with hole pockets is not easily consistent with the quantum oscillation data, because the resulting Fermi pockets are either too large or too small in area. Of course, this conclusion hinges on the applicability of the semiclassical analysis of the quantum oscillation data, which is not guaranteed for a one-band FL* state. (For a two-band FL* with asymptotically decoupled bands, such an analysis can be expected to be ok.) The fact that all pockets are hole-like also makes it difficult to explain the negative Hall coefficient, but here physics beyond weakly interacting quasiparticles might

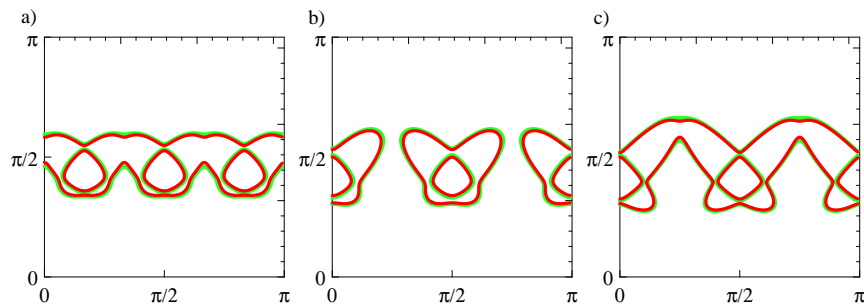


FIG. 5: Fermi surfaces (as in Fig. 1), but here for vertical charge stripes in a pseudogap state with hole pockets, the latter described by the YRZ ansatz.⁴² a) $x = 1/12$, $N = 6$, $V_c = 0.04$ eV. b) $x = 1/10$, $N = 4$, $V_c = 0.03$ eV. c) $x = 1/8$, $N = 4$, $V_c = 0.025$ eV. For details see text.

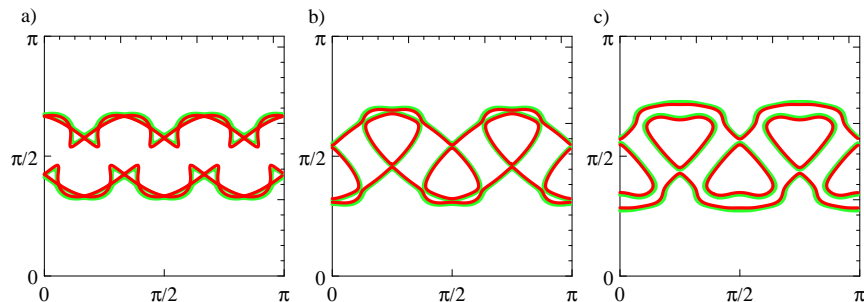


FIG. 6: Fermi surfaces for pseudogap stripes as in Fig. 5, but now for vertical spin stripes. a) $x = 1/12$, $M = 12$, $V_s = 0.035$ eV. b) $x = 1/10$, $M = 8$, $V_s = 0.035$ eV. c) $x = 1/8$, $M = 8$, $V_s = 0.05$ eV. In all cases, weak charge order is added with $V_c = V_s/10$ and $N = M/2$.

be relevant.⁹⁰

Alternatively, one could speculate about a more severe reconstruction of the FL* state by stripe formation, not captured by simply subjecting the YRZ quasiparticles to a mean-field stripe potential. This requires a thorough discussion of the interplay between stripy modulations and the driving forces of FL*, and will be presented in a forthcoming publication.

VI. DISCUSSION

In the first part of this paper, we have reviewed central aspects of stripe and nematic order in the cuprate high-temperature superconductors and connected them to observable properties in the pseudogap regime. In particular, we have critically discussed the proposal of electron pockets formed by density-wave order in a large Fermi-surface state which has been suggested to explain quantum oscillation and transport data.

Based on the fact that such descriptions do not account for full pseudogap physics – in particular, the large Fermi surface is not seen experimentally – we have suggested in the second part of this paper to investigate stripes on top of a pseudogap state. Here, we have concentrated

on states of the fractionalized-Fermi-liquid type where coherent quasiparticles populating hole pockets coexist with a spin-liquid background. Employing the YRZ description of the single-particle propagator, we have determined the Fermi surfaces of such pseudogap stripe states. These states – which now account for salient aspects of the pseudogap – can, however, not easily explain the quantum oscillation data.

This leaves us with a dilemma: Neither modulated Fermi-liquid states nor modulated pseudogap (i.e. FL*) states seem to account for the phenomenology of both quantum oscillations and the pseudogap. The following is a (certainly incomplete) list of escape routes:

- The pseudogap physics seen a zero field above T_c is entirely irrelevant for the quantum-oscillation regime at high fields and very small T . Then, a Fermi-liquid-based approach to quantum oscillations could be justified. This option would require to explain how a magnetic field of 30...50 T – still small on electronic scales – can destroy the pseudogap (which otherwise appears rather robust and is not affected⁹⁰ by fields of order 10 T).
- The low-energy fermions of the pseudogap state undergo a severe reconstruction in a magnetic field,

e.g., due to stripe formation. (Stripe formation in the quantum-oscillation regime of $\text{YBa}_2\text{Cu}_3\text{O}_y$ has been experimentally established using NMR.²¹) We note that the formation of bound states of the fractionalized constituents of FL^* is a low-energy phenomenon which could in principle be altered by moderate fields or modulations.

- The quantum oscillations do not arise from Fermi-liquid-like carriers, such that the standard Lifshitz-Kosevich analysis⁷⁸ is not applicable. This would suggest to search for quantum oscillations in other candidate pseudogap states.¹⁴¹
- Superconducting pairing cannot be neglected in the discussion of quantum oscillations. As conventional superconducting states (i.e. with a full gap or with discrete nodes) are not expected to cause quantum oscillations, one is lead to look for paired states with a Fermi surface, which appears e.g. if the condensate carries a finite momentum.^{58,91} The question of the character of the normal-conducting

pseudogap state may then be secondary.

Clearly, more experimental information would be helpful to make progress: seeing quantum oscillations in other underdoped cuprates and/or over a larger doping regime would be extremely interesting, as well as a further characterization of the stripe order in the quantum-oscillation regime (i.e. doping/field/temperature dependence of the strength and the modulation period). For theory, understanding the pseudogap – and stripe order on top of it – remains the most important issue. Among other things, it should be clarified whether and how a negative Hall coefficient may arise in hole-pocket (or Fermi-arc) states.

Acknowledgments

The author acknowledges useful discussions with A. Hackl, C. Proust, S. Sachdev, L. Taillefer, C. M. Varma, and A. Wollny. This research has been supported by the DFG through FOR 960 and GRK 1621.

-
- ¹ T. Timusk and B. W. Statt, Rep. Prog. Phys. **62**, 61 (1999).
- ² M. R. Norman, D. Pines, and C. Kallin; Adv. Phys. **54**, 715 (2005).
- ³ J. Zaanen *et al.*, Nature Phys. **2**, 138 (2006).
- ⁴ P. A. Lee, N. Nagaosa, and X.-G. Wen, Rev. Mod. Phys. **78**, 17 (2006).
- ⁵ M. R. Norman, Physics **3**, 86 (2010).
- ⁶ B. Vignolle *et al.*, C. R. Physique **12**, 446 (2011).
- ⁷ S. E. Sebastian, N. Harrison, and G. G. Lonzarich, Phil. Trans. Roy. Soc. A **369**, 1687 (2011).
- ⁸ S. Chakravarty, Rep. Prog. Phys. **74**, 022501 (2011).
- ⁹ V. J. Emery, S. A. Kivelson, and J. M. Tranquada, Proc. Natl. Acad. Sci. USA **96**, 8814 (1999).
- ¹⁰ S. A. Kivelson, I. P. Bindloss, E. Fradkin, V. Oganesyan, J. M. Tranquada, A. Kapitulnik, and C. Howald, Rev. Mod. Phys. **75**, 1201 (2003).
- ¹¹ A. H. Castro Neto and C. Morais Smith, in: Strong Interactions in Low Dimensions, D. Baeriswyl and L. Degiorgi, eds. (Kluwer, 2004), pg. 277.
- ¹² M. Vojta, Adv. Phys. **58**, 699 (2009).
- ¹³ J. M. Tranquada, B. J. Sternlieb, J. D. Axe, Y. Nakamura, and S. Uchida, Nature (London) **375**, 561 (1995).
- ¹⁴ J. M. Tranquada, J. D. Axe, N. Ichikawa, Y. Nakamura, S. Uchida, and B. Nachumi, Phys. Rev. B **54**, 7489 (1996).
- ¹⁵ P. Abbamonte, A. Rusydi, S. Smadici, G. D. Gu, G. A. Sawatzky, and D. L. Feng, Nature Phys. **1**, 155 (2005).
- ¹⁶ C. Howald, H. Eisaki, N. Kaneko, M. Greven, and A. Kapitulnik, Phys. Rev. B **67**, 014533 (2003).
- ¹⁷ M. Vershinin, S. Misra, S. Ono, Y. Abe, Y. Ando, and A. Yazdani, Science **303**, 1995 (2004).
- ¹⁸ Y. Kohsaka, C. Taylor, P. Wahl, A. Schmidt, J. Lee, K. Fujita, J. W. Alldredge, J. Lee, K. McElroy, H. Eisaki, S. Uchida, D.-H. Lee, and J. C. Davis, Science **315**, 1380 (2007).
- ¹⁹ C. V. Parker *et al.*, Nature **468**, 677 (2010).
- ²⁰ W. D. Wise, M. C. Boyer, K. Chatterjee, T. Kondo, T. Takeuchi, H. Ikuta, Y. Wang, and E. W. Hudson, Nature Phys. **4**, 696 (2008).
- ²¹ T. Wu, H. Mayaffre, S. Krämer, M. Horvatic, C. Berthier, W. N. Hardy, R. Liang, D. A. Bonn, and M.-H. Julien, Nature **477**, 191 (2011).
- ²² S. A. Kivelson, E. Fradkin, and V. J. Emery, Nature **393**, 550 (1998).
- ²³ Y. Ando, K. Segawa, S. Komiyama, and A. N. Lavrov, Phys. Rev. Lett. **88**, 137005 (2002).
- ²⁴ R. Daou *et al.*, Nature **463**, 519 (2010).
- ²⁵ V. Hinkov, D. Haug, B. Fauqué, P. Bourges, Y. Sidis, A. Ivanov, C. Bernhard, C. T. Lin, and B. Keimer, Science **319**, 597 (2008).
- ²⁶ H. Yamase and W. Metzner, Phys. Rev. B **73**, 214517 (2006).
- ²⁷ B. Edegger, V. N. Muthukumar, and C. Gros, Phys. Rev. B **74**, 165109 (2006).
- ²⁸ A. Hackl and M. Vojta, Phys. Rev. B **80**, 220514(R) (2009).
- ²⁹ B. Fauqué, Y. Sidis, V. Hinkov, S. Pailhès, C.T. Lin, X. Chaud, and P. Bourges Phys. Rev. Lett. **96**, 197001 (2006).
- ³⁰ H. A. Mook, Y. Sidis, B. Fauqué, V. Balédent, and P. Bourges, Phys. Rev. B **78**, 020506 (2008).
- ³¹ Y. Li, V. Balédent, N. Barisic, Y. Cho, B. Fauqué, Y. Sidis, G. Yu, X. Zhao, P. Bourges, and M. Greven, Nature **455**, 372 (2008).
- ³² C. M. Varma, Phys. Rev. Lett. **83**, 3538 (1999); M. E. Simon and C. M. Varma, *ibid.* **89**, 247003 (2002).
- ³³ I. Dimov, P. Goswami, X. Jia, and S. Chakravarty, Phys. Rev. B **78**, 134529 (2008).
- ³⁴ A. J. Millis and M. R. Norman, Phys. Rev. B **76**, 220503(R) (2007).
- ³⁵ J. Lin and A. J. Millis, Phys. Rev. B **78**, 115108 (2008); Phys. Rev. B **80**, 193107 (2009).

- ³⁶ M. R. Norman, J. Lin, and A. J. Millis, *Phys. Rev. B* **81**, 180513(R) (2010).
- ³⁷ A. Hackl, M. Vojta, and S. Sachdev, *Phys. Rev. B* **81**, 045102 (2010).
- ³⁸ H. Yao, D. H. Lee, and S. A. Kivelson, *Phys. Rev. B* **84**, 012507 (2011).
- ³⁹ N. Harrison, *Phys. Rev. Lett.* **102**, 206405 (2009).
- ⁴⁰ N. Harrison and S. E. Sebastian, *Phys. Rev. Lett.* **106**, 226402 (2011); N. Harrison, *ibid.* **107**, 186408 (2011).
- ⁴¹ P. W. Anderson, *Science* **235**, 1196 (1987).
- ⁴² K.-Y. Yang, T. M. Rice, and F.-C. Zhang, *Phys. Rev. B* **73**, 174501 (2006).
- ⁴³ K.-Y. Yang, T. M. Rice, and F.-C. Zhang, *Adv. Phys.* (in print).
- ⁴⁴ Y. Qi and S. Sachdev, *Phys. Rev. B* **81**, 115129 (2010).
- ⁴⁵ E. G. Moon and S. Sachdev, *Phys. Rev. B* **83**, 224508 (2011).
- ⁴⁶ T. Senthil, S. Sachdev, and M. Vojta, *Phys. Rev. Lett.* **90**, 216403 (2003).
- ⁴⁷ T. Senthil, M. Vojta, and S. Sachdev, *Phys. Rev. B* **69**, 035111 (2004).
- ⁴⁸ S. Chakravarty, R. B. Laughlin, D. K. Morr, and C. Nayak, *Phys. Rev. B* **63**, 094503 (2001).
- ⁴⁹ S. Sachdev, *Rev. Mod. Phys.* **75**, 913 (2003).
- ⁵⁰ S.-C. Zhang, *Science* **275**, 1089 (1997).
- ⁵¹ M. Vojta and S. Sachdev, *Phys. Rev. Lett.* **83**, 3916 (1999).
- ⁵² E. Demler, S. Sachdev, and Y. Zhang, *Phys. Rev. Lett.* **87**, 067202 (2001).
- ⁵³ A. Perali, C. Castellani, C. Di Castro, and M. Grilli, *Phys. Rev. B* **54**, 16216 (1996).
- ⁵⁴ J. Zaanen, O. Y. Osman, H. V. Kruis, Z. Nussinov, and J. Tworzydło, *Phil. Mag. B* **81**, 1485 (2001).
- ⁵⁵ E. Arrigoni and S. A. Kivelson, *Phys. Rev. B* **68**, 180503 (2003).
- ⁵⁶ E. Berg, E. Fradkin, E.-A. Kim, S. A. Kivelson, V. Oganesyan, J. M. Tranquada, and S. C. Zhang, *Phys. Rev. Lett.* **99**, 127003 (2007).
- ⁵⁷ Q. Li, M. Hücker, G. D. Gu, A. M. Tsvelik, and J. M. Tranquada, *Phys. Rev. Lett.* **99**, 067001 (2007).
- ⁵⁸ E. Berg, E. Fradkin, and S. A. Kivelson, *Phys. Rev. B* **79**, 064515 (2009).
- ⁵⁹ D. Haug, V. Hinkov, Y. Sidis, P. Bourges, N. B. Christensen, A. Ivanov, T. Keller, C. T. Lin, and B. Keimer, *New J. Phys.* **12**, 105006 (2010).
- ⁶⁰ V. B. Zabolotny *et al.*, *EPL* **86**, 47005 (2009).
- ⁶¹ S. R. Park *et al.*, preprint arXiv:1110.4926; D. Reznik, preprint arXiv:1202.0852.
- ⁶² J. M. Tranquada, H. Woo, T. G. Perring, H. Goka, G. D. Gu, G. Xu, M. Fujita, and K. Yamada, *Nature* **429**, 534 (2004).
- ⁶³ M. Vojta and T. Ulbricht, *Phys. Rev. Lett.* **93**, 127002 (2004).
- ⁶⁴ G. S. Uhrig, K. P. Schmidt, and M. Grüninger, *Phys. Rev. Lett.* **93**, 267003 (2004).
- ⁶⁵ M. Vojta, T. Vojta, and R. K. Kaul, *Phys. Rev. Lett.* **97**, 097001 (2006).
- ⁶⁶ G. Seibold and J. Lorenzana, *Phys. Rev. Lett.* **94**, 107006 (2005).
- ⁶⁷ H. Yamase, *Phys. Rev. B* **79**, 052501 (2009).
- ⁶⁸ K. Sun, M. J. Lawler, and E.-A. Kim, *Phys. Rev. Lett.* **104**, 106405 (2010).
- ⁶⁹ M. Vojta, *Eur. Phys. J. Special Topics* **188**, 49 (2010).
- ⁷⁰ A. Kanigel *et al.*, *Nature Phys.* **2**, 447 (2006).
- ⁷¹ H.-B. Yang, J. D. Rameau, Z.-H. Pan, G. D. Gu, P. D. Johnson, H. Claus, D. G. Hinks, and T. E. Kidd, *Phys. Rev. Lett.* **107**, 047003 (2011).
- ⁷² G. Xu *et al.*, *Nature Phys.* **5**, 642 (2009).
- ⁷³ M. Le Tacon *et al.*, *Nature Phys.* **7**, 725 (2011).
- ⁷⁴ J. L. Tallon, J. W. Loram, G. V. M. Williams, J. R. Cooper, I. R. Fisher, J. D. Johnson, M. P. Staines, and C. Bernhard, *Phys. Stat. Sol. B* **215**, 531 (1999).
- ⁷⁵ J. L. Tallon and J.W. Loram, *Physica C* **349**, 53 (2000).
- ⁷⁶ H. Alloul, J. Bobroff, M. Gabay, and P. J. Hirschfeld, *Rev. Mod. Phys.* **81**, 45 (2009).
- ⁷⁷ J. Chang *et al.*, *Phys. Rev. Lett.* **102**, 177006 (2009).
- ⁷⁸ I. M. Lifshitz and A. M. Kosevich, *Zh. Eksp. Theor. Fiz.* **29**, 730 (1955).
- ⁷⁹ B. Vignolle *et al.*, *Nature* **455**, 952 (2008).
- ⁸⁰ N. Doiron-Leyraud, C. Proust, D. LeBoeuf, J. Levallois, J.-B. Bonnemaison, R. Liang, D. A. Bonn, W. N. Hardy, and L. Taillefer, *Nature* **447**, 565 (2007).
- ⁸¹ S. E. Sebastian, N. Harrison, E. Palm, T. P. Murphy, C. H. Mielke, R. Liang, D. A. Bonn, W. N. Hardy, and G. G. Lonzarich, *Nature* **454**, 200 (2008).
- ⁸² E. A. Yelland, J. Singleton, C. H. Mielke, N. Harrison, F. F. Balakirev, B. Dabrowski, and J. R. Cooper, *Phys. Rev. Lett.* **100**, 047003 (2008).
- ⁸³ T. Helm, M. V. Kartsovnik, M. Bartkowiak, N. Bittner, M. Lambacher, A. Erb, J. Wosnitza, and R. Gross, *Phys. Rev. Lett.* **103**, 157002 (2009).
- ⁸⁴ T. Helm *et al.*, *Phys. Rev. Lett.* **105**, 247002 (2010).
- ⁸⁵ S. E. Sebastian, N. Harrison, M. M. Altarawneh, R. Liang, D. A. Bonn, W. N. Hardy, and G. G. Lonzarich, *Phys. Rev. B* **81**, 140505 (2010).
- ⁸⁶ B. J. Ramshaw, B. Vignolle, J. Day, R. Liang, W. N. Hardy, C. Proust, and D. A. Bonn, *Nature Phys.* **7**, 234 (2011).
- ⁸⁷ S. E. Sebastian, N. Harrison, M. M. Altarawneh, C. H. Mielke, R. Liang, D. A. Bonn, W. N. Hardy, and G. G. Lonzarich, *Proc. Natl. Acad. Sci. U.S.A.* **107**, 6175 (2010).
- ⁸⁸ D. LeBoeuf *et al.*, *Nature* **450**, 533 (2007).
- ⁸⁹ D. LeBoeuf *et al.*, *Phys. Rev. B* **83**, 054506 (2011).
- ⁹⁰ J. M. Tranquada, D. N. Basov, A. D. LaForge, and A. A. Schafgans, *Phys. Rev. B* **81**, 060506 (2010).
- ⁹¹ C. M. Varma, private communication.
- ⁹² M. Zelli, C. Kallin, and A. J. Berlinsky, preprint arXiv:1201.1920.
- ⁹³ M. Vojta and O. Rösch, *Phys. Rev. B* **77**, 094504 (2008).
- ⁹⁴ K. Yamada *et al.*, *Phys. Rev. B* **57**, 6165 (1998).
- ⁹⁵ S. C. Riggs, O. Vafek, J. B. Kemper, J. B. Betts, A. Migliori, F. F. Balakirev, W. N. Hardy, R. Liang, D. A. Bonn, and G. S. Boebinger, *Nature Phys.* **11**, 332 (2011).
- ⁹⁶ L. Taillefer, *J. Phys.: Condens. Matter* **21**, 164212 (2009).
- ⁹⁷ F. Laliberte *et al.*, *Nature Comm.* **2**, 432 (2011).
- ⁹⁸ V. J. Emery and S. A. Kivelson, *Nature* **374**, 434 (1995), *Phys. Rev. Lett.* **74**, 3253 (1995).
- ⁹⁹ Y. Wang, L. Li, and N. P. Ong, *Phys. Rev. B* **73**, 024510 (2006).
- ¹⁰⁰ H.-B. Yang, J. D. Rameau, P. D. Johnson, T. Valla, A. Tsvelik, and G. D. Gu, *Nature* **456**, 77 (2008).
- ¹⁰¹ A. Kanigel, U. Chatterjee, M. Randeria, M. R. Norman, G. Koren, K. Kadowaki, and J. C. Campuzano, *Phys. Rev. Lett.* **101**, 137002 (2008).
- ¹⁰² K. K. Gomes, A. N. Pasupathy, A. Pushp, S. Ono, Y. Ando, and A. Yazdani, *Nature* **447**, 569 (2007).
- ¹⁰³ Y. Wang, . Li, M. J. Naughton, G. D. Gu, S. Uchida, and N. P. Ong, *Phys. Rev. Lett.* **95**, 247002 (2005).

- ¹⁰⁴ C. Castellani, C. Di Castro, and M. Grilli, Phys. Rev. Lett. **75**, 4650 (1995).
- ¹⁰⁵ C. Castellani, C. Di Castro, and M. Grilli, J. Phys. Chem. Solids **59**, 1694 (1998).
- ¹⁰⁶ M. S. Grønseth, T. B. Nilssen, E. K. Dahl, C. M. Varma, and A. Sudbo, Phys. Rev. B **79**, 094506 (2009).
- ¹⁰⁷ B. Leridon, P. Monod, D. Colson, and A. Forget, EPL **87**, 17011 (2009).
- ¹⁰⁸ A. Macridin, M. Jarrell, T. Maier, P. R. C. Kent, and E. D’Azevedo, Phys. Rev. Lett. **97**, 036401 (2006).
- ¹⁰⁹ T. D. Stanescu, M. Civelli, K. Haule, and G. Kotliar, Ann. Physics **321**, 1682 (2006).
- ¹¹⁰ N. S. Vidhyadhiraja, A. Macridin, C. Sen, M. Jarrell, and M. Ma, Phys. Rev. Lett. **102**, 206407 (2009).
- ¹¹¹ M. Civelli, M. Capone, A. Georges, K. Haule, O. Parcollet, T. D. Stanescu, and G. Kotliar, Phys. Rev. Lett. **100**, 046402 (2008).
- ¹¹² S. Sakai, Y. Motome, and M. Imada, Phys. Rev. Lett. **102**, 056404 (2009).
- ¹¹³ P. Phillips, Ann. Phys. **321**, 1634 (2006).
- ¹¹⁴ D. Fournier *et al.*, Nature Phys. **6**, 905 (2010).
- ¹¹⁵ M. Vojta, J. Low Temp. Phys. **161**, 203 (2010).
- ¹¹⁶ M. Oshikawa, Phys. Rev. Lett. **84**, 3370 (2000).
- ¹¹⁷ M. Vojta, Phys. Rev. B **78**, 125109 (2008).
- ¹¹⁸ H.-Y. Yang, A. Läuchli, F. Mila, and K. P. Schmidt, Phys. Rev. Lett. **105**, 267204 (2010).
- ¹¹⁹ S. Yan, D. Huse, and S. R. White, Science **332**, 1173 (2011).
- ¹²⁰ H.-C. Jiang, H. Yao, and L. Balents, preprint arXiv:1112.2241.
- ¹²¹ P. Coleman, C. Pépin, Q. Si, and R. Ramazashvili, J. Phys: Condens. Matt. **13**, R723, (2001).
- ¹²² Q. Si, S. Rabello, K. Ingersent, and J. L. Smith, Nature (London) **413**, 804 (2001).
- ¹²³ C. Pépin, Phys. Rev. Lett. **98**, 206401 (2007).
- ¹²⁴ S. Biermann, L. de Medici, and A. Georges, Phys. Rev. Lett. **95**, 206401 (2005).
- ¹²⁵ S. A. Kivelson, D. S. Rokhsar, and J. P. Sethna, Phys. Rev. B **35**, 8865 (1987).
- ¹²⁶ X. G. Wen, Phys. Rev. B **44**, 2664 (1991).
- ¹²⁷ T. Senthil and M. P. A. Fisher, Phys. Rev. B **62**, 7850 (2000).
- ¹²⁸ P. Beran, D. Poilblanc, and R. B. Laughlin, Nucl. Phys. B **473**, 707 (1996).
- ¹²⁹ R. K. Kaul, Y. B. Kim, S. Sachdev, and T. Senthil, Nature Phys. **4**, 28 (2008).
- ¹³⁰ J.-W. Mei, S. Kawasaki, G.-Q. Zheng, Z.-Y. Weng, and X.-G. Wen, preprint arXiv:1109.0406.
- ¹³¹ Although a complete low-energy description of cuprates requires three bands (for the copper and oxygen orbitals), it is believed that crucial aspects like pairing and the pseudogap emerge already within a reduced one-band description.
- ¹³² It has been argued⁴² that Luttinger’s theorem can be fulfilled in a weakly doped Mott insulator with hole pockets if one considers the so-called Luttinger volume. This measures the momentum-space volume where $\text{Re}G(\mathbf{k}, \omega = 0) > 0$, which accounts for both poles and zeroes of the Green’s function. In the present discussion, we prefer to restrict our attention to the Fermi volume as defined via the poles of G , for two reasons: (i) In a two-band FL* phase zeroes do not necessarily occur in the c -electron Green’s function. (ii) As shown in Ref. 133, the Luttinger volume of a two-band Mott insulator generically violates Luttinger’s theorem in the absence of particle-hole symmetry. This result shows that zeroes of G have to be considered with care.
- ¹³³ A. Rosch, Eur. Phys. J. B **59**, 495 (2007).
- ¹³⁴ K. Haule and G. Kotliar, Phys. Rev. B **76**, 092503 (2007).
- ¹³⁵ P. Werner, E. Gull, O. Parcollet, and A. J. Millis, Phys. Rev. B **80**, 045120 (2009).
- ¹³⁶ M. Ferrero, P. S. Cornaglia, L. De Leo, O. Parcollet, G. Kotliar, and A. Georges, Phys. Rev. B **80**, 064501 (2009).
- ¹³⁷ E. Gull, M. Ferrero, O. Parcollet, A. Georges, and A. J. Millis, Phys. Rev. B **82**, 155101 (2010).
- ¹³⁸ T. Maier, M. Jarrell, T. Pruschke, and M. H. Hettler, Rev. Mod. Phys. **77**, 1027 (2005).
- ¹³⁹ R. Eder, K. Seki, and Y. Ohta, Phys. Rev. B **83**, 205137 (2011).
- ¹⁴⁰ K.-Y. Yang, H.-B. Yang, P. D. Johnson, T. M. Rice, and F.-C. Zhang, EPL **86**, 37002 (2009).
- ¹⁴¹ T. Pereg-Barnea, H. Weber, G. Refael, and M. Franz, Nature Phys. **6**, 44 (2010).